Water crystallization inside fuel cell membranes probed by X-ray scattering

Hakima Mendil-Jakani, Richard J Davies, Emilie Dubard, Armel Guillermo, Gérard Gebel

Water crystallization inside fuel cell membranes probed by X-ray scattering

Hakima Mendil-Jakani[a*], Richard J. Davies[b], Emilie Dubard[a], Armel Guillermo[a], Gérard Gebel[a]

[a] CEA Grenoble, INAC, SPrAM (UMR5819 CEA/CNRS/UJF), 17 rue des Martyrs, 38054 Grenoble Cedex 9, France
[b] ESRF, ID13, MicroFocus Beamline, 6 rue Jules Horowitz, 38043 Grenoble, France
[*] Corresponding author
Phone: 33(0)4 38 78 91 71
Fax: 33(0)4 38 78 56 91
E-mail: hakima.mendil-jakani@cea.fr

Abstract

Water properties in ionomer membranes at sub-zero temperatures are investigated as a function of water volume fraction using a micro X-Ray beam scanning the membranes along their thicknesses. The influence of both the size of confinement and the membrane nature on water behavior is analyzed. The study is focused on Nafion® membranes at different water contents to tune the size of water confinement and on water-saturated sulfonated polyimide (sPI) membrane. The scattering curves show that water does not crystallize inside Nafion® membrane up to a characteristic size of water confinement of 3 nm. Water does crystallize inside Nafion® for characteristic size of ionic domains larger than 5 nm, *i.e.* for hyperswollen state. In order to predict qualitatively the freezing occurrence of water in the Nafion® matrix, the Gibbs-Thomson model was considered; both the effect of confinement and acidity were taken into account. In this context, the water-Nafion® interfacial tension was determined using a contact angle experiment. The model is in accordance with a water crystallization occurring inside Nafion® provided that it is highly swollen. However, water behavior is also strongly dependent on the nature of the membrane. In the case of water-saturated sulfonated polyimide, a hydrocarbon based membrane, water does not crystallize upon cooling but does not desorb upon annealing in contrast to Nafion® membrane exposed to the same external conditions (temperature and relative humidity). Hence, the host-water interaction appears as a crucial parameter to take into account to describe properly the sorption-desorption and freezing phenomena.

Keywords: Nafion® membrane; sulfonated polyimide; super-cooled water; ice crystals; confinement; hyper swelling.

1. Introduction

During winter conditions, water management in proton exchange membrane fuel cells (PEMFC) is of prime importance to overcome technical challenges as the start-up at sub-zero temperatures especially for automotive applications. This is known that irreversible damages as the formation of ice in catalyst layers or inside bipolar plates induce a loss of the active layer's mechanical integrity, a delamination of the membrane electrode assembly and a sharp decrease of the electrochemical performances and prevents the start of the cell [1, 2]. Pinhole formations together with roughness and cracks have also been observed on the membrane surface [3]. In this context, the behavior of PEMFC at low temperatures has to be carefully characterized. The related ice location, *i.e.* inside [4, 5] or outside [6] the membrane is the subject of active debates. From the pioneering works of Pineri and coworkers [6], many other and strong evidences, based on infrared images of water in membrane electrode assembly [7], micro X-ray diffraction [8] and NMR measurements [9], have shown that water is in a *super-cooled* state in the membrane at temperatures below 273K and that part of the water desorbs out from the membrane, then crystallizes on its surface, but *never inside* [8]. One has reasonably expected that water cannot freeze inside Nafion® membrane since it is in a highly *confined* and *acidic* environment. When the temperature is decreased, the desorption property is driven by the ratio between the saturated vapor pressure over ice outside the membrane and the saturated vapor pressure of super-cooled water inside the membrane: this ratio is smaller than one and decreases upon cooling [9, 10].

Calorimetric experiments which show a pronounced hysteresis between the freezing and melting transitions is an argument in favor of ice location inside Nafion® nanoporosities [5].

In fact, the calorimetric experiments support our conclusions. The apparent contradiction originates from the usual interpretation of DSC thermograms that we call in question. Indeed, it has been shown by X-Ray scattering and NMR experiments that the desorption process is very slow with a kinetic of several tens of minutes up to one hour [8, 9]. The temperature scan rate typically used in standard DSC experiments (1 to 10K.min^{-1}) is clearly to fast to analyze properly the desorption process. Moreover, the re-sorption process is reversible [9]. Consequently, the wide endotherm recorded upon annealing under 273K in DSC experiments (see ex fig 3 of [5]) cannot be explained by the ice melting on the membrane surfaces but instead must be attributed to the sublimation of the thin ice layer (a few microns) throw the membrane surface occurring from low temperatures up to a temperature determined by the water concentration at 273K (see fig 7 of [9]).

In the previous X-Ray scattering study [8], the relative humidity was 100% which yields a membrane hydration, usually labeled λ for the number of water molecules per ionic site, equal to 14.

In the present paper, the range of membrane water content is first extended at both sides of λ=14 to have a global picture of water behavior inside Nafion® membranes at sub-zero temperature for low and relatively high membrane hydration. At ambient relative humidity, the Nafion® membrane hydration is low (λ≈5) which corresponds to water content sufficiently low to avoid any desorption [6, 9]. It will be shown that the direct visualization by X-Ray scattering pattern confirms the NMR analysis [9]: no water crystallization occurs and no desorption is induced by annealing. For a higher swelling state (λ≈22), obtained by thermal treatment in water at a temperature above 373K, water remains in a super cooled state at sub zero temperature. Water does not crystallize inside Nafion® membrane even when it is relatively highly swollen. Second, we will show that one has to reach *extreme condition of swelling* (λ≈51) to allow for *water crystallization inside* Nafion® membrane.

One has to keep in mind that the water content in the perfluorinated membranes has direct correlation with the characteristic size of the nanoscale separation between hydrophobic and hydrophilic domains creating a connected pore network [11, 12]. In order to predict the depression of water freezing temperature inside the porous Nafion® membranes, both the effect of water confinement and acidity are taken into account. The former is described by the Gibbs-Thomson equation where the water-Nafion® surface tension is determined by contact angle experiments. The latter is expressed by the freezing temperature of sulfuric acid which depends on the acid concentration. The combined effects of confinement and acidity support the experimental observation that water can crystallize inside Nafion® membranes provided that the *water content is very high i.e*. for low levels of water confinement and acidity.

It is also worth reminding that, at equilibrium, the water content results from a balance between osmotic pressure related to the entropy of the ionic species and the elastic energy of the polymer matrix that tends to limit the swelling. It will be shown that the matrix nature strongly influences the water sorption-desorption and freezing behaviors at low temperatures. We will present the case of a hydrocarbon membrane: a water-saturated sulfonated polyimide (sPI, λ≈9 at RH=100%) for which the water does not freeze inside sPI membrane upon cooling and does not desorb upon a subsequent annealing.

2. Experimental

2.1. Sample preparation

Nafion®117 membranes were purchased from Aldrich. The equivalent weight EW defined as the average molecular weight associated with one mole of SO_3 groups is 1100 g.equiv.$^{-1}$. The degree of sulfonation is also usually expressed as ionic exchange capacity IEC: 0.91 meq.g^{-1}. The synthesis of the sulfonated polyimide (sPI) polymer solution as well as casting, acidification and washing procedures were previously described [13, 14]. The EW of the sPI membrane is 504 g.equiv.$^{-1}$ (IEC of 1.98 meq.g^{-1}). The Nafion®117 membrane was cleaned as followed: the membrane was first soaked for 2 hrs in HNO_3 1M at 80°C to remove organic impurities and to completely acidify the membrane, and then washed in double deionized water at 80°C for 1h, to have first a reference in terms of swelling and second to remove the excess of acid. The highly swollen membranes were obtained by putting the films in a water-filled autoclave, at temperature above 373K during 12 hrs to insure swelling equilibrium. After cooling down the autoclave, the hyperswollen samples were kept in water. The membranes were then stored in water at room temperature. The polymer volume fraction Φ_p and the number of water molecules per ionic sites λ were determined gravimetrically, assuming a complete polymer–solvent phase separation following the equations [15]:

$$\Phi_p = \frac{m_p / \rho_p}{m_p / \rho_p + (m_t - m_p) / \rho_{H_2O}} \text{ and } \lambda = \frac{EW}{M_{H_2O}} * \left(\frac{m_t - m_p}{m_p} \right)$$

were m_p and m_t are the weight of the dried and swollen membrane respectively and ρ_p the polymer density which is 2.1 g.cm^{-3} and 1.4 g.cm^{-3} for Nafion® and sPI membrane respectively. At 100% RH, the number of water molecules per ionic sites λ, *i.e.* the membrane hydration , determined by water sorption isotherm is close to 14 and 9 for Nafion® and sPI membranes respectively.

2.2. Micro-X-Ray scattering set- up and geometry

Stripes of rectangular membrane (0.5–0.6 mm width, 2 cm long) were cut and introduced into a thin quartz capillary (from GLAS-Germany, 1 mm diameter). A part of the capillary was filled with water which insures a 100% relative humidity around the polymer sample. The capillary is then sealed. This capillary is mounted horizontally on a vertical translational stage in order to be scanned with the X-ray µ-beam, along the *Z*-direction, perpendicular to the plane of the membrane (see Fig.1). Scattering experiments were carried out at the ID13 microfocus beamline of the European Synchrotron Radiation Facility (ESRF,

Grenoble, France). The beamline was configured with a monochromatic X-ray beam (λ = 0.098 nm), focused using a pair of crossed linear Fresnel optics. This provided a submicron beam at the sample position of approximately 0.4 µm along both (*Y,Z*) axes which is relevant to scan the membrane thickness of about 200 µm at different height position. For data collection, a 2D high-resolution and time resolved CCD camera was mounted on a translational stage. Two-dimensional scattering spectra were recorded using 0.1 s exposures, a short acquisition time necessary to avoid X-ray beam damage and to avoid inducing unwanted temperatures changes [8]. A sample-to-film distance of 270 mm was used which corresponds to a scattering range between 1 and 19 nm^{-1} (wide angle range). All spectra collected were isotropic and an azimuthal averaging is applied to obtain a 1D scattering curve. In order to collect data at low temperatures (from 200K up to the ambient temperature), a cryoflow system using nitrogen gas from Oxford Cryosteam system (80–500K range) was used. It produces a laminar, dry and cold gas at a controlled temperature over a distance of less than 1 cm at the output of the gun; this system also avoids a water condensation on the capillary external surfaces at low temperatures. This cooler gun was mounted on a rotating support to place the output of the gun as close as possible of the extremity of the capillary. Fig. 2 shows a typical small and wide angle scattering spectrum of Nafion®117 taken at room temperature and 100% RH. The "ionomer peak", at 1.3 nm^{-1}, is characteristic of the swollen Nafion® membrane. Both the intensity and position of this peak are directly correlated to the water content of the polymer membrane [16, 17]. In the wide angle range, a broad peak is apparent around 12 nm^{-1} which contains two scattering contributions, one at 11 nm^{-1}, related to the amorphous polymer structure and the other at 12.4 nm^{-1}, related to the semi-crystalline polymeric structure [18]. The intensities and positions of these structural peaks are independent of the water content.

2.3. Contact angle experiments

Contact angle measurements were performed on Nafion® membrane with different standard probe liquids (water, diiodomethane, ethylene glycol) by sessile drop method using a Digidrop-GBX instrument goniometer. The instrument is equipped with a chamber controlled in temperature and humidity. The syringe is introduced at the top of the chamber through a small puncture. The membranes were mounted flat with double side tape on a glass slide and equilibrated in water-saturated atmosphere (100% RH, 393K) to prevent both the membrane

from buckling upon contact with water and water drop absorption by the Nafion® membrane [19]. The advancing contact angles were taken over a time period of 30 s. The Owens-Wendt two parameters model is used to determine the Nafion®-water surface tension [20].

3. Results and discussion

3.1. Nafion® membrane from λ=5 to λ=22

We first present the scattering results obtained from a quenched Nafion®117 membrane previously exposed to ambient relative humidity (47% RH), which corresponds to a water content of λ≈5. Fig.3 displays the 2D spectrum in the scattering range 1-19 nm^{-1}, taken in the transverse configuration within the membrane thickness after quenching at 200K. The strong scattering ring corresponds to the amorphous and crystalline Nafion® peaks (10-13 nm^{-1}). The typical broad peak associated to the super-cooled water (expected at 17 nm^{-1}) is not observed [21]. A subsequent annealing at 223K is performed. No evolution of the spectra taken at different time after annealing has been observed. After one hour of annealing, the membrane is scanned along its thickness to determine whether the water has desorbed. Fig.4 displays the 2D scattering patterns in the transverse configuration, respectively within the membrane thickness at different positions (Fig.4(a) and (b)) and at the membrane surface (Fig.4(c)). The surface is exempt from any ice crystals. Consequently, no water desorption has occurred during the annealing process. This *direct* observation supports the NMR analysis: below λ=7, no desorption of liquid water occurs during cooling and consequently no crystalline water is expected onto the Nafion® membrane surfaces [6, 9]. Water does not crystallize inside Nafion® membrane up to at least λ≈18, *i.e.* for a polymer volume fraction of Φ_p=64% [9]. The distance *d* between the elongated polymer aggregates extracted from the position of the ionomer peak q_{iono}, $d = \frac{2\pi}{q_{iono}}$, is about 5 nm. The available space for water location, extracted from the extrapolation of data reporting $d(\Phi_p)$, is $d_w=d-d_0\approx 2$ nm with $d_0\approx 3$ nm the typical distance for a dry membrane [22]. It appears that this water confinement prevents the water crystallization. It is expected that water crystallize for a higher degree of swelling inside the Nafion® membrane.

At room temperature in water, the water uptake corresponds to λ≈18. To increase the water content, the Nafion® membrane is submitted to a heating stage in water at temperature above 373K (see the experimental section). The sample studied contains 57% vol. fraction of polymer, which corresponds to λ≈22. The sample being highly swollen, the corresponding ionomer peak is shifted to a q range not accessible with the μ X-Ray beam. The characteristic

distance between polymer aggregates deduced from previous studies is about 6 nm which corresponds to a space for water location of $d_w \approx 3$ nm [22]. Is this size of confinement sufficient to obtain ice inside Nafion® membrane at sub zero temperatures? The sample was quenched at 200K. Fig. 5(a) displays a series of 2D scattering from the capillary with the beam shining out and through the membrane along its thickness (see Fig.5(a), (A) (B) and (J) for spectra outside the membrane, (C) to (I) for spectra inside the membrane). Fig. 5(b) displays the 1D scattering plot taken within the membrane at the (E) position as shown by the typical amorphous and crystalline Nafion® peak located in the range (10-13 nm^{-1}). In the wide angle range (15-19 nm^{-1}), a large and triangular peak, which is the signature of super cooled water, is observed [21]. Some individual ice crystals are localized on the surfaces and outside the membrane as shown by the bright spots observed in Fig.5(a) (B) (C) and (J) due to a partial water desorption. The degree of swelling is high but not sufficient to observe water crystallization inside Nafion® membrane. In the following, the sample studied is in a very high swelling state.

3.2. Hyperswollen Nafion® membrane at $\lambda \approx 51$

The volumic fraction of polymer is about 36% corresponding to $\lambda \approx 51$. This sample contains almost three fold water molecules per ionic sites compared to a water-saturated Nafion® membrane. The characteristic distance between fibrillar aggregates is very large and about 8 nm [22]. The space for water location is about 5 nm: twice and half as much as in a water saturated Nafion® membrane at room temperature [22]. The sample was first quenched at 200K. Fig.6 displays a series of two-dimensional spectra taken along the membrane thickness at different heights (separated by 15 µm). The water is not in the frozen state, but in contrast in the *crystalline* state inside the membrane [23]. The degree of swelling is high enough to allow for water crystallization inside the membrane. The powder diffraction signature of Fig 6(a) (J) shows that a partial water desorption has occurred. The high water content of the membrane may involve the segregation of the highly charged domains and consequently the formation of large water filled inter-fibrillar regions, where the water can crystallize. It would be worth predicting the temperature depression of water freezing within the porous Nafion® matrix. Both the effect of water confinement and acidity are taken into account. The effect of confinement on water freezing is well described and modeled by the well-known Gibbs-Thomson equation in ordered mesoporous silica and alumina materials [24]:

$$\Delta T = T_f - T = \frac{2T_f V_m \gamma_{SL}}{\frac{d_w}{2}\Delta H_f} \qquad (1)$$

where $\Delta T=T_f-T$ is the temperature depression: T_f is the bulk freezing temperature, T that in the pores, d_w is the size of water confinement, ΔH_f is the molar melting enthalpy, V_m is the molar volume of water, and γ_{SL} is the solid-water surface tension (where *S* and *L* stand for "solid" and "liquid" respectively).

Perfluorosulfonated membranes absorb a quantity of water tuned by the ambient relative humidity which yields to a characteristic pore size [12, 22]. Upon quenching, the membrane structure does not change and both water and polymer chains are dynamically "frozen" [8]. Hence, the Gibbs-Thomson concept appears relevant to analyze quantitatively the water freezing depression inside the pores of Nafion® matrix.

The Nafion®-water surface tension γ_{SL}, which was up to now the missing parameter, is determined in the following. The determination of a drop profile on a flat surface provides a simple and efficient tool to quantify the affinity between a liquid and a substrate. This observation has been translated by the Young's equation in the early 19th century [25]:

$$\gamma_{SL} = \gamma_{SV} - \gamma_{LV}\cos\theta \quad (2)$$

where γ_{SL}, γ_{SV} and γ_{LV} are the solid-liquid, solid-vapor and liquid-vapor surface tension respectively, θ is the contact angle of a drop of liquid deposited on a solid surface. While θ and γ_{LV} can be easily determined, γ_{SL} and γ_{SV} remain unknown with the unique Young equation. Numerous theories have been derived to determine the missing parameters depending on the surface chemistry [26]. We use the Owens-Wendt two-parameter calculation where the surface tension γ_{LV} and γ_{SV} are the sum of a polar component (p) a dispersive (d) one for the van der Waals type interactions [20, 26]:

$$\gamma_{LV} = \gamma_{LV}^{d} + \gamma_{LV}^{p} \quad (3)$$

$$\gamma_{SV} = \gamma_{SV}^{d} + \gamma_{SV}^{p} \quad (4)$$

Starting from Good's equation [27]:

$$\gamma_{SL} = \gamma_{SV} + \gamma_{LV} - 2\left[\sqrt{\gamma_{SV}^{d}\gamma_{LV}^{d}} + \sqrt{\gamma_{SV}^{p}\gamma_{LV}^{p}}\right] \quad (5)$$

and combining with Young's equation (2) gives:

$$(1+\cos\theta)\frac{\gamma_{LV}^{p}+\gamma_{LV}^{d}}{2\sqrt{\gamma_{LV}^{d}}} = \sqrt{\gamma_{SV}^{d}} + \sqrt{\gamma_{SV}^{p}} \times \sqrt{\frac{\gamma_{LV}^{p}}{\gamma_{LV}^{d}}} \quad (6)$$

The two components γ_{SV}^{d} and γ_{SV}^{p} (which are the missing parameters of eq. (5) to determine γ_{SL}) can be determined by plotting $(1+\cos\theta)\frac{\gamma_{LV}^{p}+\gamma_{LV}^{d}}{2\sqrt{\gamma_{LV}^{d}}}$ as a function of $\sqrt{\gamma_{LV}^{p}/\gamma_{LV}^{d}}$ with the

measured contact angle θ of standard probe liquids with known values of γ_{LV}^{d} and γ_{LV}^{p}. Table 1 gathers the contact angles of the probe liquids together with the corresponding surface tension components γ_{LV}^{d} and γ_{LV}^{p} .

Table 1. Contact angles (293K) for water, diiodomethane and ethylene glycol on Nafion®117 membrane surface in a water-saturated atmosphere (RH=100%).

liquid	Advancing contact angle θ°	γ_{LV}^{d} (mN.m^{-1})$^{(a)}$	γ_{LV}^{p} (mN.m^{-1})$^{(b)}$
Water	98±2°	21.8	51
Ethylene glycol	76±2°	29	19
Diiodomethane	74±2°	50.8	0

(a) (b) *Source: Digidrop processor tensiometer database*

The contact angle θ=98° of water drop on Nafion® surface (100% RH) is in accordance with that found in the literature [28]. Typically, uncertainties within 2° are obtained for the contact angles. Fig.7 displays the Owens-Wendt plot based on Eq. (6) obtained with the three testing fluids. The polar and dispersive components deduced are γ_{SV}^{d} =20.2 mN.m^{-1} and γ_{SV}^{p} =2 mN.m^{-1} respectively. Finally, the Nafion®-water surface tension can be determined and is about γ_{SL}=32.9±1.1 mN.m^{-1} (eq. (5)). The calculated depression of water freezing temperature as a function of the pore diameter is plotted in Fig. 8. using the values for water at its normal freezing temperature, T_f=273K, V_m=18 cm^3.mol^{-1} an ΔH_f =6 kJ.mol^{-1}.

An effect of acidity on the freezing depression temperature of water in acidic Nafion® was estimated and added to the confinement property alone. The freezing point of the mixture H_2SO_4/H_2O was chosen. It depends on the acid concentration and is depicted in the phase diagram reported in ref. [29]. The region in grey in Fig. 8 represents the range of pore size and temperature depression where it has been shown experimentally that water does not crystallize inside Nafion® membrane [6, 9]. According to this model, it is predicted that water cannot crystallize in a water-saturated Nafion® membrane at λ=18 which is experimentally observed. The depression of freezing temperature expected for water in the confined and acidic environment defined by Nafion® porosity is about ΔT=52K and ΔT=25K in pore size of 3 nm and 5 nm respectively (λ≈22 and λ≈51). A temperature stage at ΔT=70K would have yield to a water freezing in Nafion® at λ≈22 but is not observed experimentally. It can be reasonably explained by a confinement size near the theoretical limit (2.5 nm). On the contrary, for the sample swollen at λ≈51 where the size d_w≈5 nm is twice larger than the limit value, the

observation of a water crystallization inside Nafion® membrane by X-Ray scattering well agrees with the temperature depression model. However, while X-Ray scattering is an efficient tool for the determination of water and ice location, the quantitative study of water crystallization by NMR as a function of membrane water content over a wide range of λ values is under progress.

At this stage, one can wonder if the water properties at low temperatures are a general trend shared by all ionomer membranes. In the following part, we present results related to the quenching and annealing of a water-saturated sulfonated polyimide (sPI) membrane, characterized by a rigid hydrocarbon polymer backbone.

3.3. Water-saturated sulfonated polyimide membrane.

The sPI membrane differs from the benchmark perfluorosulfonated Nafion® membrane in many aspects. The polymer backbone of sPI is a hydrocarbon block copolymer composed of ionic sequences spaced by hydrophobic sequences. The bulky naphthalenic groups confer a rigid structure to the polymer chain associated to a very high glass transition temperature above 570K [30]. The glassy nature of the polymer matrix limits the dimensional changes associated to water uptake [13]. The sPI membrane exposed to a water-saturated atmosphere reaches $\lambda \approx 9$ [30]. Fig.9 (a) displays a 2D spectrum recorded within the sPI membrane thickness at ambient temperature at 100% RH. In this scattering range (1.5-18 nm^{-1}), no structural peaks associated to the polymer matrix are observed because they are not accessible for the micro-SAXS experiment. Small angle spectra revealed a broad maximum on an intense small-angle upturn located at very low angles compared to perfluorosulfonated systems [13]. This scattering maximum was attributed to the ionomer peak since such a peak is commonly observed with ionomers [31] but is still the subject of controversy [32]. The associated interdomain distance of about 25 nm is typically 5 to 10 times larger than in Nafion®. Upon hydration, the scattering intensity increases but the peak position remains unchanged [13], *i.e.*, the contrast increases while the local structure is not modified. These two observations can be reconciled by an explanation in terms of water filling of pre-existing porosities, created during the membrane preparation process, which does not affect the local structure. This behavior is singular compared to the case of Nafion® where the scattering intensity increase is observed together with the shift of the ionomer peak position towards small angles.

At large angles, the behavior presents an important deviation from the typical q^{-4} Porod's law usually observed for ion conducting membranes. A q^{-4} behavior at larges angles indicates a sharp interface between water contained in the ionic domains and the polymer matrix. The

deviation for sPI membrane can hardly be explained by a smooth interface but rather by an internal structuration inside the ionic domains [30]. Indeed, the micro-SAXS also revealed a scattering peak at 4.5 nm^{-1} corresponding to a characteristic distance of 1.5 nm but at low relative humidity only [33]. This scattering contribution comes from the spatial repetition of ionic groups in the ionic sequence.

The membrane is quenched at 200K. The 2D scattering spectrum is displayed in Fig.9 (b). Despite the interdomain distances of sPI membrane are very large (d≈25 nm), water does not freeze in the water-saturated sPI. This result is in opposition with the water crystallization observed inside Nafion® membrane for typical size of water confinement of d_w≈5 nm. What can explain this surprising behavior? This behavior is likely to be related to the internal structure of the hydrophilic domains and to the water affinity with respect to the polymer matrix which may yield to an actual space for water (d_w confinement size) smaller than that expected from d≈25 nm.

Besides, it has been shown by field-cycling NMR relaxometry that water interacts strongly with the hydrophilic groups at the interface of the sPI matrix which is typical of a good wetting situation while a non-wetting situation is observed in the case of Nafion® [34]. This water-host affinity is explained by the hydrocarbon type backbone and the high content of oxygen atoms. This statement is supported by the specific two-step hydration mechanisms for sPI membrane derived from infrared absorption spectroscopy [35]: upon hydration of the ionic and the polar groups of the polymer, the percolation threshold at λ≈5 is not reached until the first water layer, necessary for a long range transport, has been adsorbed onto the whole surface. This strong water-polymer chain interaction is in accordance with the low conductivity measured before λ≈5 contrasting with the much higher one in Nafion® membrane [36].

The membrane was then annealed for one hour at 223K. Fig.10 displays the 2D scattering patterns in the transverse configuration, respectively within the membrane thickness at two different positions, separated by 20µm height (Fig.10 (a) and (b)) and at the membrane surface (Fig.10 (c)). Water does not desorb during the annealing process at 223K since water crystals are not observed at the membrane surface. The swelling-deswelling properties at ambient temperature have been analyzed by sorption isotherms that revealed a strong hysteresis between the sorption and desorption properties [30]. This observation was first attributed to a very low desorption process [37]. The equilibration time was then varied for each data point up to 12 hrs and the hysteresis was still observed [30]. The extrapolation of the kinetic to infinite equilibration time clearly ascertains that the hysteresis is related to a true physical property of

the sPI membrane. The strong water-matrix interaction goes against water desorption since part of the water interact strongly with the polar groups of the polymer chains and helps in maintaining the water inside the membrane.

4. Conclusions

We have performed micro X-Ray experiments to investigate the structure of water at sub zero temperatures inside two kinds of ionomer membranes: Nafion® and sulfonated polyimide. X-Ray spectra show that for Nafion® membrane exposed to ambient relative humidity, *i.e.* at $\lambda \approx 5$, water does not freeze in the membrane and does not desorb upon annealing which confirms the results obtained by the NMR analysis [6, 9]. Water remains in a frozen state and does not crystallize upon quenching up to high water content of $\lambda \approx 22$, *i.e.* for size of water confinement of 3 nm but desorbs [9].

We have shown that one has to reach very high swelling state as $\lambda \approx 51$, obtained by a thermal treatment at elevated temperature, to allow for water crystallization inside Nafion®. The typical size of water confinement is 5 nm and the level of acidity is low. The Nafion®-water surface tension was determined by contact angle experiments to model the depression of water freezing inside Nafion®, considering both the effect of confinement and acidity. We confirm that the conditions to observe ice inside Nafion® are a strong water swelling and correlatively a low ionic concentration. These observations contrast with the statements that water can crystallize inside Nafion® membrane swollen at room temperature [4, 5].

The case of a hydrocarbon based sPI membrane was studied. While the membrane is water-saturated and the ionic domains are large, water does not freeze upon cooling. We have also observed that despite water remains liquid-like, it does not desorb upon annealing. This specific and singular behavior has been interpreted in terms of an interplay between a strong water-membrane affinity and the internal structure of the ionic domains that both prevent water crystallization and water desorption.

Finally, the observation of the specific behavior of sPI membranes is of practical interest for fuel cell operating conditions at low temperatures. The absence of water desorption and subsequent crystallization on catalyst layers represents a promising alternative and a supplementary argument to replace perfluorosulfonated membranes by hydrocarbon based membranes. However, previous fuel cell tests in PEMFCs have shown a low chemical stability [30]. Finally, designing hydrocarbon based membranes with rigid backbone that can prevent

both water desorption at low temperatures and membrane degradation represents an exciting challenge to overcome in this low-temperature application.

Acknowledgments

We acknowledge Céline Cailleteau and Sandrine Dourdain for fruitful discussions.

References

[1] R. Borup, J. Meyers, B. Pivovar, Y. S. Kim, R. Mukundan, N. Garland, D. Myers, M. Wilson, F. Garzon, D. Wood, P. Zelenay, K. More, K. Stroh, T. Zawodzinski, J. Boncella, J. E. McGrath, M. Inaba, K. Miyatake, M. Hori, K. Ota, Z. Ogumi, S. Miyata, A. Nishikata, Z. Siroma, Y. Uchimoto, K. Yasuda, K. I. Kimijima, N. Iwashita, Scientific aspects of polymer electrolyte fuel cell durability and degradation, Chemical Reviews 107 (2007) 3904-3951.
[2] E. Pinton, Y. Fourneron, S. Rosini, L. Antoni, Experimental and theoretical investigations on a proton exchange membrane fuel cell starting up at subzero temperatures, Journal of Power Sources 186 (2009) 80-88.
[3] Q. G. Yan, H. Toghiani, Y. W. Lee, K. W. Liang, H. Causey, Effect of sub-freezing temperatures on a PEM fuel cell performance, startup and fuel cell components, Journal of Power Sources 160 (2006) 1242-1250.
[4] M. Saito, K. Hayamizu, T. Okada, Temperature dependence of ion and water transport in perfluorinated ionomer membranes for fuel cells, Journal of Physical Chemistry B 109 (2005) 3112-3119.
[5] E. L. Thompson, T. W. Capehart, T. J. Fuller, J. Jorne, Investigation of low-temperature proton transport in Nafion using direct current conductivity and differential scanning calorimetry, J Electrochem Soc 153 (2006) A2351-A2362;
J. Lin, P.-H. Wu, R. Wycisk, P. N. Pintauro, Z. Shi, Properties of Water in Prestretched Recast Nafion, Macromolecules 41 (2008) 4284-4289.
[6] M. Pineri, F. Volino, M. Escoubes, Evidence for Sorption Desorption Phenomena during Thermal Cycling in Highly Hydrated Perfluorinated Membranes, Journal of Polymer Science Part B-Polymer Physics 23 (1985) 2009-2020.
[7] Y. Ishikawa, T. Morita, K. Nakata, K. Yoshida, M. Shiozawa, Behavior of water below the freezing point in PEFCs, Journal of Power Sources 163 (2007) 708-712.
[8] M. Pineri, G. Gebel, R. J. Davies, O. Diat, Water sorption-desorption in Nafion (R) membranes at low temperature, probed by micro X-ray diffraction, Journal of Power Sources 172 (2007) 587-596.
[9] A. Guillermo, G. Gebel, H. Mendil-Jakani, E. Pinton, NMR and Pulsed Field Gradient NMR Approach of Water Sorption Properties in Nafion at Low Temperature, Journal of Physical Chemistry B 113 (2009) 6710-6717.
[10] K. G. Gallagher, B. S. Pivovar, T. F. Fuller, Electro-osmosis and water uptake in polymer electrolytes in equilibrium with water vapor at low temperatures, ECS Trans, 16 (2008) 297-307.
[11] S. Schlick, Ionomers: Characterization, Theory and Application, CRC Press: Boca Raton, 1996.
[12] K. A. Mauritz, R. B. Moore, State of understanding of Nafion, Chemical Reviews 104 (2004) 4535-4585.
[13] N. Cornet, O. Diat, G. Gebel, F. Jousse, D. Marsacq, R. Mercier, M. Pineri, Sulfonated polyimide membranes: a new type of ion-conducting membrane for electrochemical applications, J New Mat Elect Syst 3 (2000) 33-42.
[14] C. Genies, R. Mercier, B. Sillion, R. Petiaud, N. Cornet, G. Gebel, M. Pineri, Stability study of sulfonated phthalic and naphthalenic polyimide structures in aqueous medium, Polymer 42 (2001) 5097-5105.
[15] D. R. Morris, X. D. Sun, Water-Sorption and Transport-Properties of Nafion-117-H, Journal of Applied Polymer Science 50 (1993) 1445-1452.
[16] L. Rubatat, G. Gebel, O. Diat, Fibrillar structure of Nafion: Matching Fourier and real space studies of corresponding films and solutions, Macromolecules 37 (2004) 7772-7783.
[17] K. Schmidt-Rohr, Q. Chen, Parallel cylindrical water nanochannels in Nafion fuel-cell membranes, Nature Materials 7 (2008) 75-83.

[18] P. C. van der Heijden, L. Rubatat, O. Diat, Orientation of drawn Nafion at molecular and mesoscopic scales, Macromolecules 37 (2004) 5327-5336.
[19] S. Goswami, S. Klaus, J. Benziger, Wetting and absorption of water drops on nafion films, Langmuir 24 (2008) 8627-8633.
[20] D. K. Owens, R. C. Wendt, Estimation of Surface Free Energy of Polymers, Journal of Applied Polymer Science 13 (1969) 1741-&.
[21] I. Kohl, E. Mayer, A. Hallbrucker, The glassy water-cubic ice system: a comparative study by X-ray diffraction and differential scanning calorimetry, Phys Chem Chem Phys 2 (2000) 1579-1586.
[22] G. Gebel, Structural evolution of water swollen perfluorosulfonated ionomers from dry membrane to solution, Polymer 41 (2000) 5829-5838.
[23] B. J. Murray, D. A. Knopf, A. K. Bertram, The formation of cubic ice under conditions relevant to Earth's atmosphere, Nature 434 (2005) 202-205.
[24] H. K. Christenson, Confinement effects on freezing and melting, J Phys-Condens Mat 13 (2001) R95-R133.
[25] C. J. van Oss, Development and applications of the interfacial tension between water and organic or biological surfaces, Colloid Surface B 54 (2007) 2-9.
[26] A. W. Adamson, A. P. Gast, Physical Chemistry of Surfaces, 6th, Wiley, New York, 2007.
[27] R. J. Good, L. A. Girifalco, A Theory for Estimation of Surface and Interfacial Energies .3. Estimation of Surface Energies of Solids from Contact Angle Data, Journal of Physical Chemistry 64 (1960) 561-565.
[28] T. A. Zawodzinski, S. Gottesfeld, S. Shoichet, T. J. Mccarthy, The Contact-Angle between Water and the Surface of Perfluorosulfonic Acid Membranes, J Appl Electrochem 23 (1993) 86-88.
[29] K. D. Beyer, A. R. Hansen, M. Poston, The search for sulfuric acid, J Phys Chem A 107 (2003) 2025-2032.
[30] C. Marestin, G. Gebel, O. Diat, R. Mercier, Sulfonated Polyimides, Adv Polym Sci 216 (2008) 185-258.
[31] W. Essafi, G. Gebel, R. Mercier, Sulfonated polyimide ionomers: A structural study, Macromolecules 37 (2004) 1431-1440.
[32] G. Gebel, O. Diat, Neutron and x-ray scattering: Suitable tools for studying ionomer membranes, Fuel Cells 5 (2005) 261-276.
[33] J. F. Blachot, O. Diat, J. L. Putaux, A. L. Rollet, L. Rubatat, C. Vallois, M. Muller, G. Gebel, Anisotropy of structure and transport properties in sulfonated polyimide membranes, Journal of Membrane Science 214 (2003) 31-42.
[34] J. C. Perrin, S. Lyonnard, A. Guillermo, P. Levitz, Water dynamics in ionomer membranes by field-cycling NMR relaxometry, Journal of Physical Chemistry B 110 (2006) 5439-5444.
[35] D. Jamroz, Y. Marechal, Hydration of sulfonated polyimide membranes. II. Water uptake and hydration mechanisms of protonated homopolymer and block copolymers, Journal of Physical Chemistry B 109 (2005) 19664-19675.
[36] Y. Yin, J. H. Fang, T. Watari, K. Tanaka, H. Kita, K. Okamoto, Synthesis and properties of highly sulfonated proton conducting polyimides from bis(3-sulfopropoxy)benzidine diamines, J Mater Chem 14 (2004) 1062-1070.
[37] T. Watari, H. Y. Wang, K. Kuwahara, K. Tanaka, H. Kita, K. Okamoto, Water vapor sorption and diffusion properties of sulfonated polyimide membranes, Journal of Membrane Science 219 (2003) 137-147.

Figure captions

Fig.1. Scattering geometry with the membrane enclosed in a quartz capillary. The Z-axis corresponds to the scan direction with the μ X-ray beam.

Fig.2. Typical log-log SA-WAXS curve from a swollen Nafion® membrane with characteristic peaks.

Fig.3. 2D spectrum from Nafion® exposed to ambient relative humidity and quenched at 200K, in the transverse configuration, within the membrane thickness.

Fig.4. 2D spectrum from Nafion® along its thickness (a) and (b) and at its surface (c) after one hour of annealing at 223K.

Fig.5. (a) Series of 2D scattering from the capillary with the beam shining out and through the membrane containing ≈22 water molecules per ionic sites, along its thickness. The white parts correspond to the more intense region in terms of scattering ((A) (B) and (J): outside the membrane, (C) to (I) inside the membrane thickness). Some spots which are the signature of several ice crystals are observed on the membrane surface. (b) Log-log 1D scattering plot taken within the membrane at the (E) position.

Fig.6. (a) Series of 2D scattering from the capillary with the beam shining out and through the membrane containing ≈51 water molecules per ionic sites, along its thickness. ((A) and (J): outside the membrane, (B) to (I) inside the membrane thickness). (b) Log-log 1D scattering plot taken within the membrane at the (E) position.

Fig.7. Owens-Wendt plot for Nafion® membrane. The polar and dispersive components deduced from the slope and from the ordinate after extrapolation are γ_{SV}^{d} =20.2 mN.m^{-1} and γ_{SV}^{p} =2 mN.m^{-1} respectively.

Fig.8. Depression of the freezing temperature ΔT of water (dotted and brown line) and of the mixture H_2SO_4/H_2O (straight and red line) in Nafion® as a function of the pore diameter d_w. The region in grey represents the range of pore size and temperature where it has been shown experimentally that water does not freeze inside Nafion®.

Fig.9. (a) 2D scattering from the water saturated sulfonated polyimide membrane at room temperature in the transverse configuration, within the membrane thickness and (b) quenched at 200K.

Fig.10. 2D scattering from sPI along its thickness (a) and (b) and at its surface (c) after an annealing of one hour at 223K.

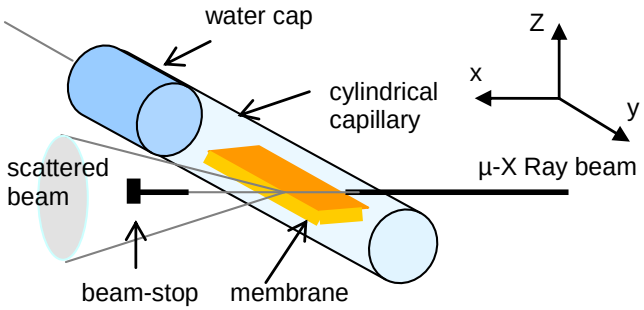
water cap
cylindrical
capillary
Z
x
y
scattered
beam
μ-X Ray beam
beam-stop
membrane

Fig.1

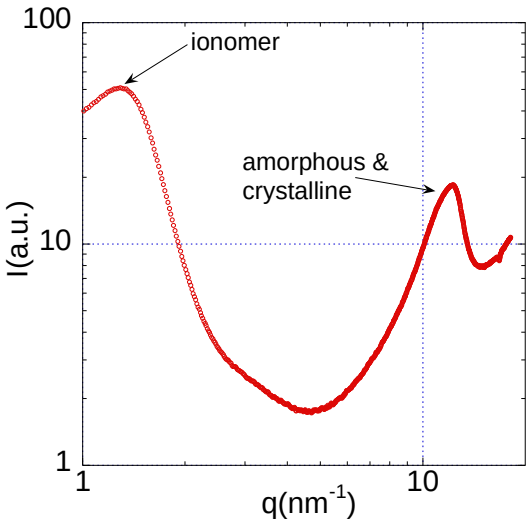
100
10
1
I(a.u.)
ionomer
amorphous &
crystalline
1
10
q(nm-1)

Fig.2

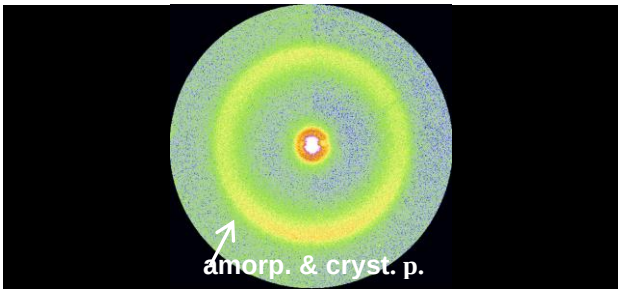
amorp. & cryst. p.

Fig.3

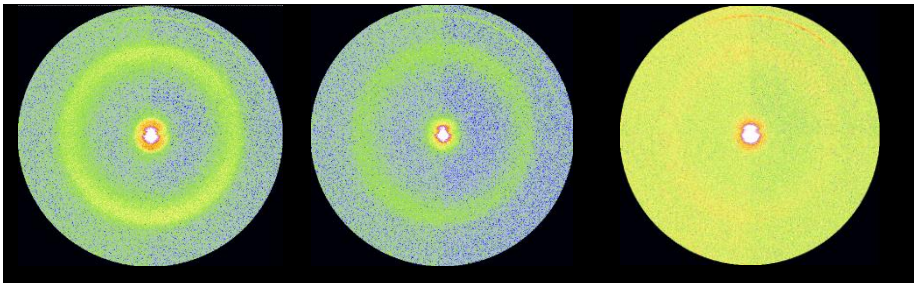

(a) Membrane thickness (b) Membrane surface (c)

Fig.4

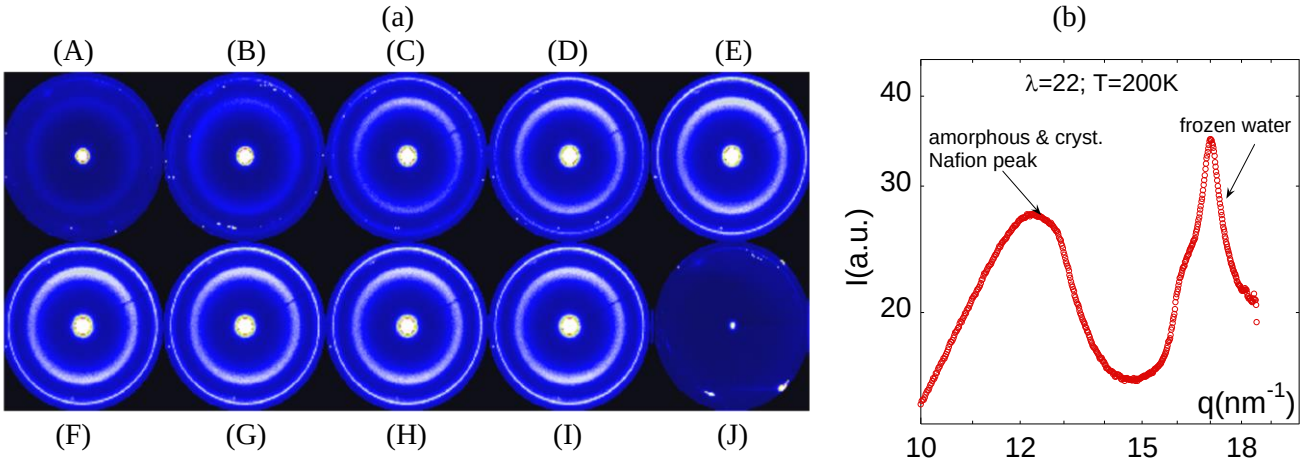

Fig.5

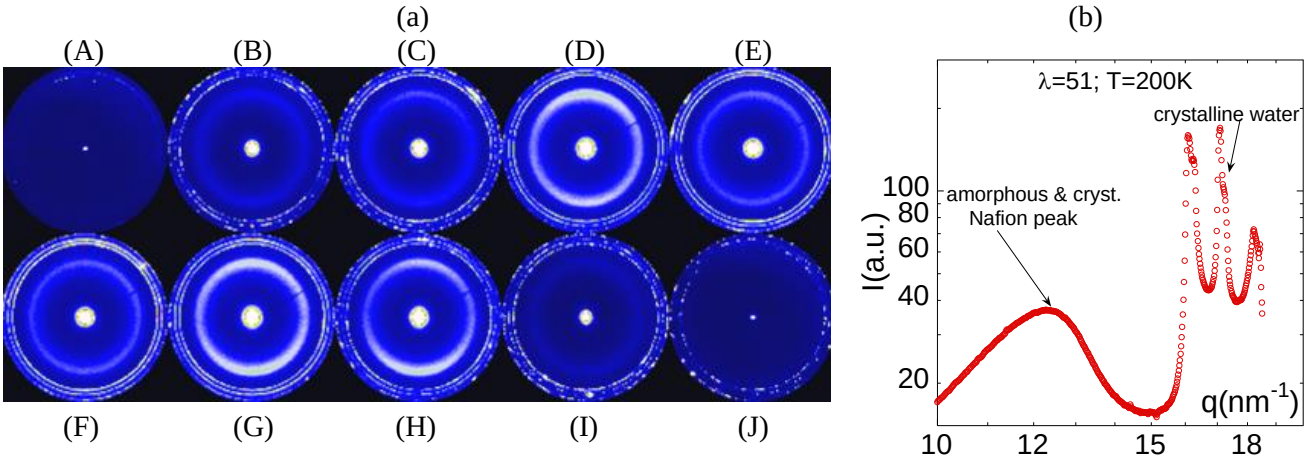

Fig.6

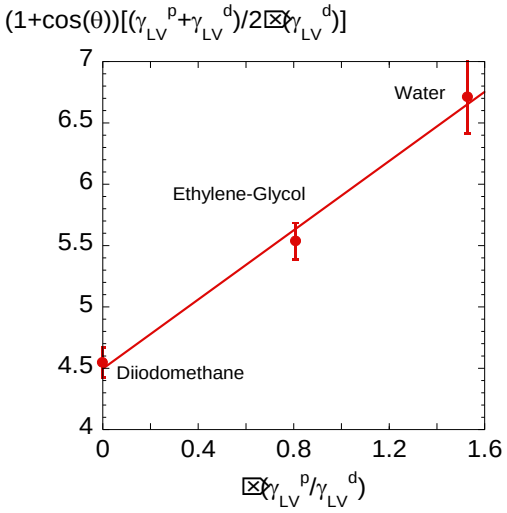

Fig.7

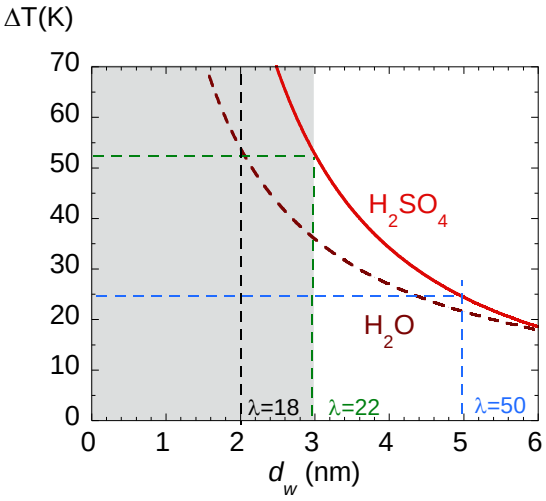

Fig.8

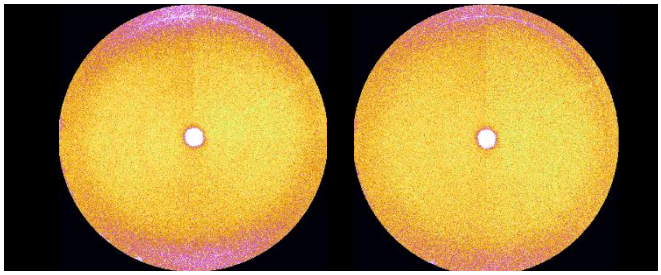

(a) Ambient Temperature (b) 200K

Fig.9

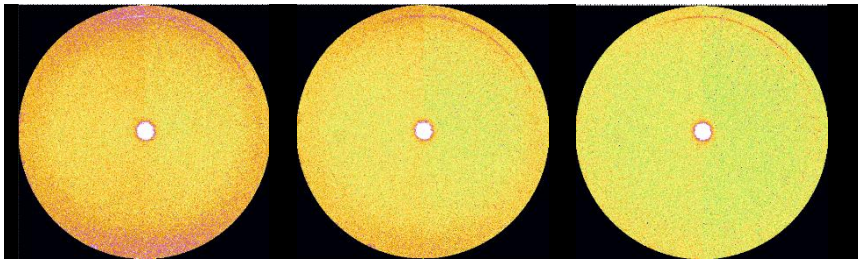

(a) Membrane thickness (b) (c) Membrane surface

Fig.10